

**Genuine tripartite continuous-variable entanglement with spatial degrees of freedom of photons**A. T. Avelar<sup>1,\*</sup> and S. P. Walborn<sup>2,†</sup><sup>1</sup>*Instituto de Física, Universidade Federal de Goiás, Caixa Postal 130, Goiânia, GO 74.001-970, Brazil*<sup>2</sup>*Instituto de Física, Universidade Federal do Rio de Janeiro, Caixa Postal 68528, Rio de Janeiro, RJ 21941-972, Brazil*

(Received 15 July 2013; published 10 September 2013)

We propose an experimentally feasible scheme to prepare tripartite continuous-variable entanglement with the spatial degrees of freedom of photons. The scheme relies on postselection upon the state obtained when one photon of an entangled pair produced by spontaneous parametric down-conversion interferes with a single photon on a 50:50 beam splitter. We show that the presence of genuine tripartite entanglement can be detected by the van Loock–Furusawa criterion.

DOI: [10.1103/PhysRevA.88.032308](https://doi.org/10.1103/PhysRevA.88.032308)

PACS number(s): 03.67.Bg, 05.45.Yv, 03.75.Lm, 42.65.Tg

**I. INTRODUCTION**

In addition to being a fundamental feature that distinguishes quantum systems from classical systems [1], quantum entanglement is also a promising resource for the transmission and processing of information. Quantum information protocols such as quantum teleportation [2], dense coding [3], and quantum key distribution [4] offer distinct advantages over classical schemes. Even though it is more difficult to create, multipartite entanglement provides a direct way to extend quantum information protocols to an arbitrary number of parties and enables a richer set of applications such as quantum secret sharing [5], resolution of the Byzantine agreement protocol [6], and one-way quantum computation [7]. The progress of quantum information science is closely connected to our abilities to generate multipartite entangled states.

Although historically the first proposal of an entangled state was made in the context of the seminal Einstein-Podolsky-Rosen paper [8] with position and momentum continuous variables (CVs) of particles, the subsequent development of quantum information in discrete variables has progressed quite rapidly, partly due to the fact that there are a number of systems more convenient for experimental realization. Typically, the experimental implementation of CV quantum information tasks is done with the quadrature operators of the quantized modes of the electromagnetic field [9] rather than the position and momentum of particles. In this context, tripartite entanglement has been created between the pump and two down-converted fields directly from an optical parametric oscillator [10] and, previously, by entangling squeezed vacuum modes on beam splitters [11].

In a different experimental context, the spatial variables of single photons have some experimental advantages such as high-quality entanglement available with spontaneous parametric down-conversion (SPDC) in nonlinear media and coincidence counting, flexibility and robustness in the quantum-state engineering by using masks, gratings, and spatial light modulators [12,13]. Furthermore, many interesting experimental results have been achieved with spatial CVs such as observation of spatial antibunching [14,15] and nonlocal optical vortices [16,17], simulation of nonlocal

Popescu-Rohrlich correlations [18], and detection of EPR steering correlations [19–23], all of them employing only bipartite CV entanglement. In most situations, the nonlinear crystal is pumped with a Gaussian pump beam, and the entanglement is well characterized by witnesses of Gaussian entanglement [19,24–26]. However, there has been some work on producing and characterizing spatially non-Gaussian entangled states [27].

There has been some effort to produce CV entanglement in the time and frequency degrees of freedom of three photons using cascaded SPDC [28], and theoretical studies have shown that entangled photon triples can be produced by third-order SPDC [29,30]. Moreover, CV entangled states of three or more photons have been studied in the context of quantum imaging [31,32] and genuine tripartite entanglement [33]. This work has considered three photon states produced from multiphoton down-conversion in nonlinear media. It has also been shown that stimulated emission of photon pairs from SPDC produces four-photon spatial entanglement [34].

In discrete degrees of freedom such as polarization, entanglement of more than two photons is typically created by producing two or more pairs of entangled photons and interfering with one photon from each pair on a beam splitter [35,36]. The multipartite entanglement appears in the postselection of events where the photons leave different outputs in the beam splitter. Here we show that the two-photon interference between one photon of a spatially entangled pair and a third photon can also be used to produce genuine tripartite CV entanglement in the spatial degrees of freedom of three photons. We present a scheme that is feasible with current technology. The proposal opens new possibilities towards the realization of more elaborate quantum information processing.

This paper is organized as follows. In Sec. II we propose a feasible experimental setup to produce tripartite CV entanglement with spatial degrees of freedom of SPDC photons. In Sec. III we introduce the van Loock–Furusawa criteria based on the variances of position and momentum linear combinations, which are sufficient conditions to detect genuine multipartite entanglement. Finally, we present our conclusions in Sec. IV.

**II. EXPERIMENTAL PROPOSAL**

Figure 1 exhibits the type of experimental setup we consider. A pulsed pump laser is used to produce two pairs of

\*avelar@ufg.br

†swalborn@if.ufjf.br

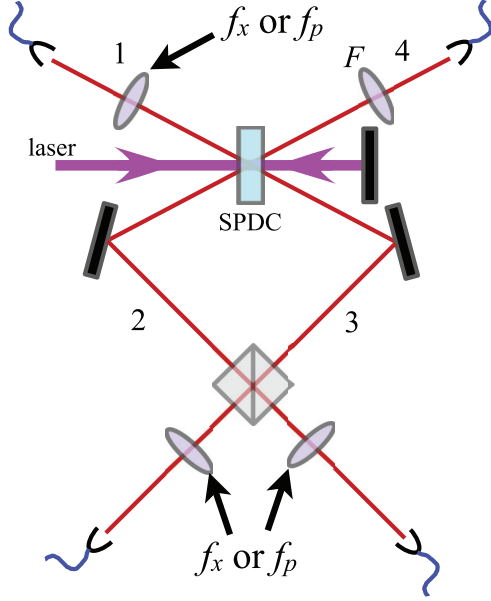


FIG. 1. (Color online) Proposed experiment. SPDC in a nonlinear crystal produces spatially entangled photon pairs. Photons 2 and 3 are combined on a 50:50 beam splitter. Photon 4 is used as a trigger to signal a single photon in path 3. A lens  $F$  is used to map the far-field distribution of photon 4 onto the detection plane. Lenses of focal lengths  $f_x$  and  $f_p$  can be used to measure the near-field ( $x$ ) or far-field ( $p$ ) distributions of photons 1, 2, and 3. Lenses  $f_x$  are used to map the image of the crystal plane onto the detection planes, while lenses  $f_p$  map the Fourier distribution (far field) onto the detection planes.

photons via SPDC in a BBO crystal in a forward-and-backward setup [12], creating two pairs of spatially entangled photons. We consider only the spatial degrees of freedom of the photons. Experimentally, this corresponds to using spectral filters to guarantee that the photons are narrow bandwidth and using a crystal configuration such that the photons are in a separable polarization state. At each output face of the SPDC crystal, the down-converted photons are described to good approximation by the quantum state [12]

$$|\psi\rangle_{ij} = \int d\mathbf{q}_i d\mathbf{q}_j v_{ij}(\mathbf{q}_i + \mathbf{q}_j) \gamma_{ij}(\mathbf{q}_i - \mathbf{q}_j) |\mathbf{q}_i\rangle |\mathbf{q}_j\rangle, \quad (1)$$

where the index  $ij$  refers to the entangled pairs,  $ij = 12$  and  $ij = 34$ , and  $\mathbf{q}_i$  and  $\mathbf{q}_j$  are the transverse wave vectors of the down-converted photons  $i$  and  $j$ , respectively. Assuming that the pump laser has a Gaussian transverse profile, the angular spectrum function  $v_{ij}(\mathbf{q})$  is

$$v_{ij}(\mathbf{q}_i + \mathbf{q}_j) = \frac{1}{\sqrt{\pi} \sigma_{ij}} \exp\left[-\frac{\sigma_{ij}^2}{4} |\mathbf{q}_i + \mathbf{q}_j|^2\right]. \quad (2)$$

Here  $\sigma_{ij}$  is given by the waist of the pump beam and can be precisely controlled using optical lens systems. The phase-matching function is  $\gamma_{ij}(\mathbf{q}) \propto \text{sinc}(a q^2)$ , where  $a$  depends upon the crystal length and wave number of the pump beam. For a thin crystal, this function is well approximated by a

Gaussian function [37]. Thus, we consider

$$\gamma_{ij}(\mathbf{q}_i - \mathbf{q}_j) = \frac{1}{\sqrt{\pi} \delta_{ij}} \exp\left[-\frac{\delta_{ij}^2}{4} |\mathbf{q}_i - \mathbf{q}_j|^2\right]. \quad (3)$$

The width  $\delta_{ij}$  of the phase-matching function is determined by the length of the crystal and the wavelength of the pump beam [12] and can be controlled by changing the crystal length. Since in this Gaussian approximation state (1) is separable in Cartesian coordinates, the entanglement is characterized by the Schmidt number  $K = K_x * K_y$ , where  $K_x = K_y = (\sigma^2 + \delta^2)/2\sigma\delta$  refer to the entanglement in  $x$  and  $y$  transverse spatial coordinates [38].

Photon 4 is used as a trigger for a single-photon state in path 3, and we consider fourfold coincidence events at the four detectors in the four paths. Including the trigger photon 4 in these events essentially removes the events where two photon pairs are created in either paths 1 and 2 or paths 3 and 4, and zero photons in the other paths. In the path of photon 4 is an optical system consisting of a lens of focal length  $F$ , which implements a Fourier transform from the crystal face to the detection plane. Detection of photon 4 at position  $\rho$  in the detection plane projects photon 4 onto momentum state  $\mathbf{q} = k\rho/F$ , where  $k$  is the wave number of photon 4 [20]. Thus, using a point detector at  $\rho = 0$  projects photon 4 onto  $\mathbf{q} = 0$ , which postselects the state

$$|\psi\rangle_{34} = \int d\mathbf{q}_3 v_{34}(\mathbf{q}_3) \gamma_{34}(\mathbf{q}_3) |\mathbf{q}_3\rangle. \quad (4)$$

Assuming that  $\delta_{34} \ll \sigma_{34}$ , so that  $\gamma_{34}(\mathbf{q}_3)$  is constant in the region where  $v_{34}(\mathbf{q}_3)$  is appreciable, we have

$$|\psi\rangle_3 = |\psi\rangle_{34} = \int d\mathbf{q}_3 \phi(\mathbf{q}_3) |\mathbf{q}_3\rangle, \quad (5)$$

where  $\phi(\mathbf{q}_3) \propto v_{34}(\mathbf{q}_3)$ .

Photons 2 and 3 are combined at a 50:50 nonpolarizing beam splitter, with path lengths aligned so that two-photon Hong-Ou-Mandel interference will occur [39]. We postselect interference events so that only coincidence detections at detectors 1, 2, and 3 are considered. After the beam splitter and with the postselection the total state  $|\Psi\rangle_T$  reads

$$|\Psi\rangle_T = \int d\mathbf{q}_1 d\mathbf{q}_2 \mathbf{q}_3 v(\mathbf{q}_1 + \mathbf{q}_2) \gamma(\mathbf{q}_1 - \mathbf{q}_2) \phi(\mathbf{q}_3) \times [|\mathbf{q}_1, \mathbf{q}_2, \mathbf{q}_3\rangle - |\mathbf{q}_1, \mathbf{q}'_3, \mathbf{q}'_2\rangle], \quad (6)$$

where the prime indicates that the  $y$  component has its sign inverted due to reflection at the beam splitter [40,41].

In transverse wave-vector space, the wave function is

$$\Psi(\mathbf{q}_1, \mathbf{q}_2, \mathbf{q}_3) = \frac{1}{N_q} \left[ \exp\left(-\frac{\sigma^2}{4} |\mathbf{q}_1 + \mathbf{q}_2|^2 - \frac{\delta^2}{4} |\mathbf{q}_1 - \mathbf{q}_2|^2 - \epsilon^2 |\mathbf{q}_3|^2\right) - \exp\left(-\frac{\sigma^2}{4} |\mathbf{q}_1 + \mathbf{q}'_3|^2 - \frac{\delta^2}{4} |\mathbf{q}_1 - \mathbf{q}'_3|^2 - \epsilon^2 |\mathbf{q}'_3|^2\right) \right], \quad (7)$$

where, for simplicity, we define  $\sigma = \sigma_{12}$ ,  $\delta = \delta_{12}$ , and  $\epsilon = \sigma_{34}$ . The normalization constant is

$$N_q = \frac{\pi^3}{\sigma^2 \delta^2 \epsilon^2} \left[ 1 - \frac{16\sigma^2 \delta^2 \epsilon^2}{(\sigma^2 + \delta^2 + 4\epsilon^2)(\sigma^2 \delta^2 + \sigma^2 \epsilon^2 + \delta^2 \epsilon^2)} \right]. \quad (8)$$

Now, taking the Fourier transform of the wave function, (7), we obtain the position-space wave function

$$\begin{aligned} \Phi(\rho_1, \rho_2, \rho_3) &= \frac{1}{N_\rho} \left[ \exp\left(-\frac{|\rho_1 + \rho_2|^2}{4\sigma^2} - \frac{|\rho_1 - \rho_2|^2}{4\delta^2} - \frac{|\rho_3|^2}{4\epsilon^2}\right) \right. \\ &\quad \left. - \exp\left(-\frac{|\rho_1 + \rho_3|^2}{4\sigma^2} - \frac{|\rho_1 - \rho_3|^2}{4\delta^2} - \frac{|\rho_3|^2}{4\epsilon^2}\right) \right], \quad (9) \end{aligned}$$

with the normalization constant

$$N_\rho = 4\pi^3 \sigma^2 \delta^2 \epsilon^2 \times \left[ 1 - \frac{16\sigma^2 \delta^2 \epsilon^2}{(\sigma^2 + \delta^2 + 4\epsilon^2)(\sigma^2 \delta^2 + \sigma^2 \epsilon^2 + \delta^2 \epsilon^2)} \right]. \quad (10)$$

For simplicity, let us consider only one spatial dimension, so we integrate the wave function, (7), in  $y$  components of the transverse direction, resulting in

$$\begin{aligned} \mathcal{P}(\vec{p}) &= \frac{1}{N_q} \{A_1 \exp(-\vec{p}^T B_1 \vec{p}) - 2A_2 \exp(-\vec{p}^T B_2 \vec{p}) \\ &\quad + A_1 \exp(-\vec{p}^T B_3 \vec{p})\}, \quad (11) \end{aligned}$$

where the vector  $\vec{p}^T = (p_1, p_2, p_3)$  has the wave vector in the  $x$  direction as its components, and

$$A_1 = \pi^{3/2} / \sqrt{2\sigma\delta\epsilon}, \quad (12)$$

$$A_2 = \sqrt{\frac{8\pi^3}{(\sigma^2 + \delta^2 + 4\epsilon^2)(\sigma^2 \delta^2 + \sigma^2 \epsilon^2 + \delta^2 \epsilon^2)}}, \quad (13)$$

$$B_1 = \begin{pmatrix} \frac{\sigma^2 + \delta^2}{2} & \frac{\sigma^2 - \delta^2}{2} & 0 \\ \frac{\sigma^2 - \delta^2}{2} & \frac{\sigma^2 + \delta^2}{2} & 0 \\ 0 & 0 & 2\epsilon^2 \end{pmatrix}, \quad (14)$$

$$B_2 = \begin{pmatrix} \frac{\sigma^2 + \delta^2}{2} & \frac{\sigma^2 - \delta^2}{4} & \frac{\sigma^2 - \delta^2}{4} \\ \frac{\sigma^2 - \delta^2}{4} & \frac{\sigma^2 + \delta^2}{4} + \epsilon^2 & 0 \\ \frac{\sigma^2 - \delta^2}{4} & 0 & \frac{\sigma^2 + \delta^2}{4} + \epsilon^2 \end{pmatrix}, \quad (15)$$

$$B_3 = \begin{pmatrix} \frac{\sigma^2 + \delta^2}{2} & 0 & \frac{\sigma^2 - \delta^2}{2} \\ 0 & 2\epsilon^2 & 0 \\ \frac{\sigma^2 - \delta^2}{2} & 0 & \frac{\sigma^2 + \delta^2}{2} \end{pmatrix}. \quad (16)$$

We note that matrix  $B_1$  ( $B_3$ ) contains correlations between photon 1 and photon 2 (photon 1 and photon 3), while matrix  $B_2$  describes possible correlations among all three photons.

Doing the same integration in the wave function, (9), we obtain

$$\begin{aligned} \mathcal{P}(\vec{x}) &= \frac{1}{N_\rho} \{\tilde{A}_1 \exp(-\vec{x}^T \tilde{B}_1 \vec{x}) - 2\tilde{A}_2 \exp(-\vec{x}^T \tilde{B}_2 \vec{x}) \\ &\quad + \tilde{A}_1 \exp(-\vec{x}^T \tilde{B}_3 \vec{x})\}, \quad (17) \end{aligned}$$

where the vector  $\vec{x}^T = (x_1, x_2, x_3)$  has the position in the  $x$  direction as its components, and

$$\tilde{A}_1 = \sqrt{2\pi^3 \sigma \delta \epsilon}, \quad (18)$$

$$\tilde{A}_2 = \frac{4\sqrt{2\pi^3 \sigma^2 \delta^2 \epsilon^2}}{\sqrt{(\sigma^2 + \delta^2 + 4\epsilon^2)(\sigma^2 \delta^2 + \sigma^2 \epsilon^2 + \delta^2 \epsilon^2)}}, \quad (19)$$

$$\tilde{B}_1 = \begin{pmatrix} \frac{1}{2} \left( \frac{1}{\sigma^2} + \frac{1}{\delta^2} \right) & \frac{1}{2} \left( \frac{1}{\sigma^2} - \frac{1}{\delta^2} \right) & 0 \\ \frac{1}{2} \left( \frac{1}{\sigma^2} - \frac{1}{\delta^2} \right) & \frac{1}{2} \left( \frac{1}{\sigma^2} + \frac{1}{\delta^2} \right) & 0 \\ 0 & 0 & \frac{1}{2\epsilon^2} \end{pmatrix}, \quad (20)$$

$$\tilde{B}_2 = \begin{pmatrix} \frac{1}{2} \left( \frac{1}{\sigma^2} + \frac{1}{\delta^2} \right) & \frac{1}{4} \left( \frac{1}{\sigma^2} - \frac{1}{\delta^2} \right) & \frac{1}{4} \left( \frac{1}{\sigma^2} - \frac{1}{\delta^2} \right) \\ \frac{1}{4} \left( \frac{1}{\sigma^2} - \frac{1}{\delta^2} \right) & \frac{1}{4} \left( \frac{1}{\sigma^2} + \frac{1}{\delta^2} + \frac{1}{\epsilon^2} \right) & 0 \\ \frac{1}{4} \left( \frac{1}{\sigma^2} - \frac{1}{\delta^2} \right) & 0 & \frac{1}{4} \left( \frac{1}{\sigma^2} + \frac{1}{\delta^2} + \frac{1}{\epsilon^2} \right) \end{pmatrix}, \quad (21)$$

$$\tilde{B}_3 = \begin{pmatrix} \frac{1}{2} \left( \frac{1}{\sigma^2} + \frac{1}{\delta^2} \right) & 0 & \frac{1}{2} \left( \frac{1}{\sigma^2} - \frac{1}{\delta^2} \right) \\ 0 & \frac{1}{2\epsilon^2} & 0 \\ \frac{1}{2} \left( \frac{1}{\sigma^2} - \frac{1}{\delta^2} \right) & 0 & \frac{1}{2} \left( \frac{1}{\sigma^2} + \frac{1}{\delta^2} \right) \end{pmatrix}. \quad (22)$$

Here, again, matrix  $\tilde{B}_2$  describes the possible tripartite correlations, while the other two matrices describe bipartite correlations. Figure 2 shows several plots of the marginal probability distributions corresponding to the tripartite quantum state, obtained by integrating the tripartite probability distributions, (17) and (11), over one of the variables. Figure 2(a) shows the distribution  $P(p_1, p_+)$ , where  $p_\pm = \frac{p_2}{2} \pm \frac{p_3}{2}$ . We see that the state is highly squeezed in these variables, showing an anticorrelation. There is also an oscillation along the antidiagonal direction, due to interference of the two wave packets corresponding to the two coincidence events at the

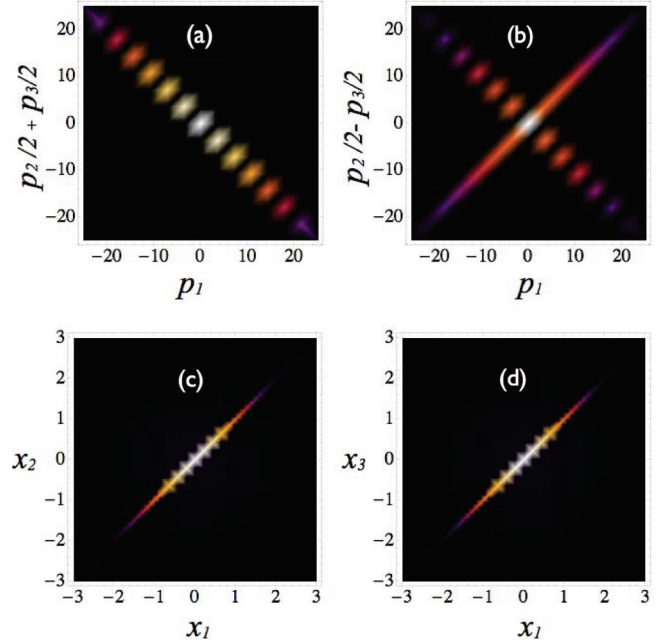


FIG. 2. (Color online) Density plots of marginal probability distributions of the tripartite quantum state. Here  $\sigma = 1.7$ ,  $\delta = 1.7/40$ , and  $\epsilon = 0.9$ .

beam splitter. Figure 2(b) shows the distribution  $P(p_1, p_-)$ , which shows essentially no correlation. Figures 2(c) and 2(d) show distributions  $P(x_1, x_2)$  and  $P(x_1, x_3)$ , respectively. We see that there is a strong correlation in both of these plots, again, with oscillations, this time along the diagonal direction. Since correlations are indeed present between several variables in both the  $x$  and the  $p$  representations, we expect that tripartite entanglement is present. We show this explicitly in the next section.

### III. GENUINE TRIPARTITE ENTANGLEMENT

To identify genuine tripartite entanglement, one can apply the van Loock–Furusawa criterion [42], which furnishes sufficient conditions for genuine multipartite entanglement. According to [42], sufficient conditions for genuine multipartite entangled states are obtained by violating, for appropriate linear combinations of the position  $\hat{x}_i$  and momentum  $\hat{p}_i$  operators for each degree of freedom  $i$  with  $[\hat{x}_i, \hat{p}_j] = \delta_{ij}$ , the inequalities of the total variance

$$\langle(\Delta\hat{u})^2\rangle_\rho + \langle(\Delta\hat{v})^2\rangle_\rho \geq f(h_1, h_2, \dots, h_N, g_1, g_2, \dots, g_N), \quad (23)$$

where  $\langle(\Delta\hat{\xi})^2\rangle = \langle\hat{\xi}^2\rangle - \langle\hat{\xi}\rangle^2$  represents the variance,  $\hat{u} \equiv h_1\hat{x}_1 + h_2\hat{x}_2 + \dots + h_N\hat{x}_N$ ,  $\hat{v} \equiv g_1\hat{p}_1 + g_2\hat{p}_2 + \dots + g_N\hat{p}_N$ , and  $f(\dots)$  stands for the boundaries of the total variance conditions. Here the  $g_j$ 's and  $h_j$ 's are arbitrary real numbers that define the global variables  $u$  and  $v$ . In the case of our scheme, once the marginal distributions  $\mathcal{P}(\vec{p})$  and  $\mathcal{P}(\vec{x})$  are determined experimentally, we can optimize over these parameters for maximal violation of inequality (23). Appropriate linear combinations are given by those where

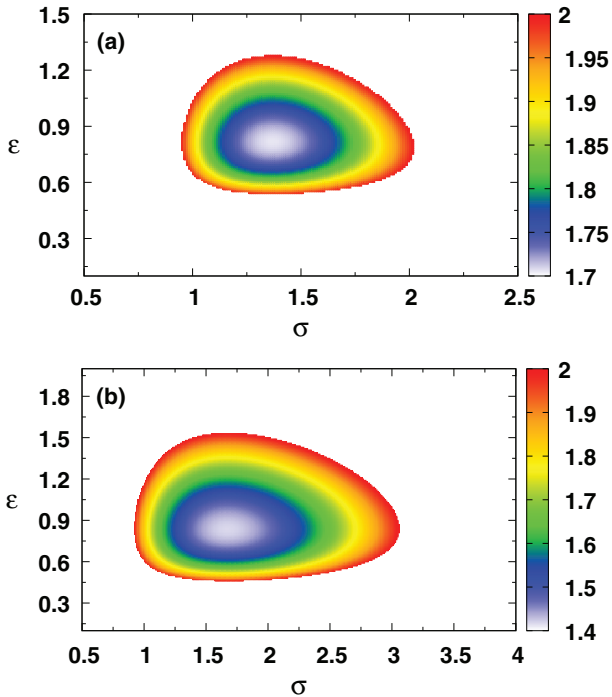


FIG. 3. (Color online) Values of  $\sigma$  and  $\epsilon$  that violate the van Loock–Furusawa criterion for (a)  $\delta = \sigma/4$  and (b)  $\delta = \sigma/40$ .

$f(\dots) \neq 0$ ,  $[\hat{u}, \hat{v}] = 0$ . To be practical, one must employ the following procedure [42]: after selecting a distinct bipartition  $(\vec{i}, \vec{N} - \vec{i})$ , choose appropriate  $\hat{u}$  and  $\hat{v}$ , ruling out all possible separable splittings between this pairing of sets of modes in the convex sum of the total density operators. Finally, consider different bipartitions  $(\vec{i}, \vec{N} - \vec{i})$  in order to negate all partial separabilities.

In the particular case of a tripartite system, the van Loock–Furusawa criteria imply that genuine tripartite entanglement is identified if any pair of the following inequalities is violated simultaneously:

$$\begin{aligned} \Delta_{12} &= \langle[\Delta(\hat{x}_1 - \hat{x}_2)]^2\rangle + \langle[\Delta(g_1\hat{p}_1 + \hat{p}_2 + g_3^{\text{opt}}\hat{p}_3)]^2\rangle \geq 2, \\ \Delta_{23} &= \langle[\Delta(\hat{x}_2 - \hat{x}_3)]^2\rangle + \langle[\Delta(g_1^{\text{opt}}\hat{p}_1 + \hat{p}_2 + \hat{p}_3)]^2\rangle \geq 2, \\ \Delta_{13} &= \langle[\Delta(\hat{x}_1 - \hat{x}_3)]^2\rangle + \langle[\Delta(\hat{p}_1 + g_2^{\text{opt}}\hat{p}_2 + \hat{p}_3)]^2\rangle \geq 2, \end{aligned} \quad (24)$$

where  $g_1^{\text{opt}}$ ,  $g_2^{\text{opt}}$ , and  $g_3^{\text{opt}}$  are optimized parameters.

Using Eqs. (11) and (17) and the definition of variance we have

$$\begin{aligned} \langle(\Delta\hat{u})^2\rangle &= \int d\vec{x} (\vec{x}^T D_u \vec{x}) \mathcal{P}(\vec{x}) \\ &= \frac{\pi^{2/3}}{2N_\rho} \left[ \tilde{A}_1 \frac{\text{tr}(D_u \tilde{B}_1^{-1})}{\sqrt{\det \tilde{B}_1}} - 2\tilde{A}_2 \frac{\text{tr}(D_u \tilde{B}_2^{-1})}{\sqrt{\det \tilde{B}_2}} \right. \\ &\quad \left. + \tilde{A}_1 \frac{\text{tr}(D_u \tilde{B}_3^{-1})}{\sqrt{\det \tilde{B}_3}} \right], \quad (25) \\ \langle(\Delta\hat{v})^2\rangle &= \int d\vec{p} (\vec{p}^T D_v \vec{p}) \mathcal{P}(\vec{p}) \\ &= \frac{\pi^{2/3}}{2N_q} \left[ A_1 \frac{\text{tr}(D_v B_1^{-1})}{\sqrt{\det B_1}} - 2A_2 \frac{\text{tr}(D_v B_2^{-1})}{\sqrt{\det B_2}} \right. \\ &\quad \left. + A_1 \frac{\text{tr}(D_v B_3^{-1})}{\sqrt{\det B_3}} \right], \quad (26) \end{aligned}$$

where the matrices  $D_u$  and  $D_v$ , defining the appropriate combinations, are given by

$$D_u = \begin{pmatrix} h_1^2 & h_1 h_2 & h_1 h_3 \\ h_1 h_2 & h_2^2 & h_2 h_3 \\ h_1 h_3 & h_2 h_3 & h_3^2 \end{pmatrix} \quad (27)$$

and

$$D_v = \begin{pmatrix} g_1^2 & g_1 g_2 & g_1 g_3 \\ g_1 g_2 & g_2^2 & g_2 g_3 \\ g_1 g_3 & g_2 g_3 & g_3^2 \end{pmatrix}. \quad (28)$$

Inequalities (24) are obtained setting  $h_1 = 1, h_2 = -1, h_3 = 0, g_1 = 1, g_2 = 1, g_3 = g_3^{\text{opt}}$  for  $\Delta_{12}$ ,  $h_1 = 0, h_2 = 1, h_3 = -1, g_1 = g_1^{\text{opt}}, g_2 = 1, g_3 = 1$  for  $\Delta_{23}$ , and  $h_1 = 1, h_2 = 0, h_3 = -1, g_1 = 1, g_2 = g_2^{\text{opt}}, g_3 = 1$  for  $\Delta_{13}$ , respectively.  $\Delta_{12} = \Delta_{13}$  are violated for colored regions of parameters shown in Fig. 3 as a function of  $\sigma$  and  $\epsilon$ . In all cases,  $g_j^{\text{opt}}$  is optimized for maximum violation. We present results for  $\delta = \sigma/4$  and  $\delta = \sigma/40$ , corresponding to initial bipartite entanglement quantified by Schmidt numbers  $K_x = 2.125$  and

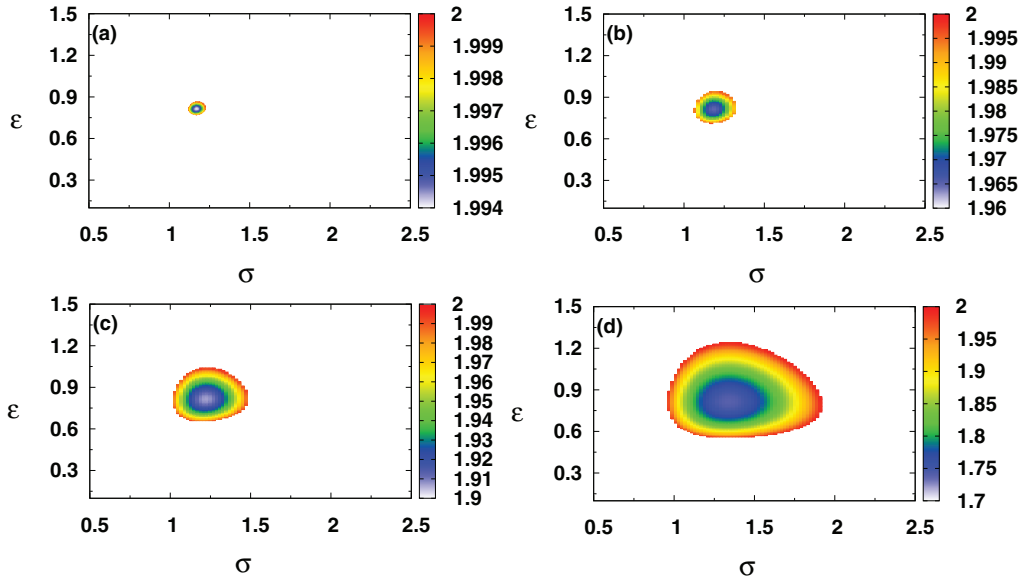


FIG. 4. (Color online) Values of  $\sigma$  and  $\epsilon$  that violate the van Loock–Furusawa criterion for (a)  $\delta = \sigma/2.5$ , (b)  $\delta = \sigma/2.6$ , (c)  $\delta = \sigma/2.8$ , and (d)  $\delta = \sigma/(2 + \sqrt{3})$ .

$K_x \approx 20$ , respectively. The color scale shows the value of  $\Delta_{12} = \Delta_{13}$ , which is less than the lower bound of 2 for a range of parameters that grows with the entanglement  $K_x$ .

Figure 4 shows the violation of inequalities (24) near the region of no violation. For  $\sigma > \delta$ , violation begins when  $\delta \approx \sigma/2.49$ , which corresponds to a Schmidt number of  $K_x \approx 1.45$ . The region of parameters for violation increases with the ratio  $\sigma/\delta$ . For  $\delta = \sigma/(2 + \sqrt{3})$ , we have a Schmidt number  $K_x = 2$ , which is equal to a pure maximally entangled state of two-qubits, or one ebit of entanglement.

#### IV. DISCUSSION AND CONCLUSIONS

In conclusion, in this paper we propose a scheme to generate genuine tripartite CV entangled states based on the spatial degrees of freedom of photons produced by SPDC. The genuine tripartite entanglement can be verified experimentally via the van Loock–Furusawa entanglement criteria [42]. Our proposal should be realizable with current technology, as four-photon experiments using SPDC have been reported in the literature for roughly 15 years. The correlations in position and wave vector can be measured by using optical lens systems to map the near-field and far-field distributions onto the detector planes [19,20,25], as illustrated in Fig. 1. The wave-vector

distribution corresponds to the far-field distribution of the source and is typically mapped using a  $2f$  optical system, which implements the optical Fourier transform. The position distributions correspond to the near-field distributions of the source and can be mapped onto the detection planes using imaging systems. We note that the longitudinal positioning of these lenses is somewhat critical, so that the proper field distribution is mapped onto the detection planes. This is particularly true for optical systems with small-focal-length lenses. In this regard, it is advantageous to employ lenses with larger values of  $f$  ( $> 100$  cm), as has been done in recent work [19,20,25]. Once the appropriate field distribution is mapped onto the detection plane, the fourfold intensity correlations can be measured by scanning the detectors in the transverse plane [19,20,25] or using recently available EMCCD or ICCD cameras [43], which can register photon coincidence events. The present proposal opens new perspectives in CV quantum information processing.

#### ACKNOWLEDGMENTS

The authors would like to acknowledge financial support from the Brazilian agencies CAPES (PROCAD), CNPq, FAPERJ, and INCT-Informação Quântica.

- [1] E. Schrödinger, *Naturwissenschaften* **23**, 807 (1935).
- [2] C. H. Bennett, G. Brassard, C. Crépeau, R. Jozsa, A. Peres, and W. K. Wootters, *Phys. Rev. Lett.* **70**, 1895 (1993).
- [3] C. H. Bennett and S. J. Weisner, *Phys. Rev. Lett.* **69**, 2881 (1992).
- [4] A. K. Ekert, *Phys. Rev. Lett.* **67**, 661 (1991).
- [5] M. Hillery, V. Buzek, and A. Berthiaume, *Phys. Rev. A* **59**, 1829 (1999).

- [6] M. Fitzi, N. Gisin, and U. Maurer, *Phys. Rev. Lett.* **87**, 217901 (2001).
- [7] R. Raussendorf and H. J. Briegel, *Phys. Rev. Lett.* **86**, 5188 (2001).
- [8] A. Einstein, D. Podolsky, and N. Rosen, *Phys. Rev.* **47**, 777 (1935).
- [9] S. L. Braunstein and P. van Loock, *Rev. Mod. Phys.* **77**, 513 (2005).

- [10] A. S. Coelho, F. A. S. Barbosa, K. N. Cassemiro, A. S. Villar, M. Martinelli, and P. Nussenzveig, *Science* **326**, 823 (2009).
- [11] T. Aoki, N. Takei, H. Yonezawa, K. Wakui, T. Hiraoka, A. Furusawa, and P. van Loock, *Phys. Rev. Lett.* **91**, 080404 (2003).
- [12] S. P. Walborn, C. H. Monken, S. Pádua, and P. H. Souto Ribeiro, *Phys. Rep.* **495**, 87 (2010).
- [13] D. S. Tasca, R. M. Gomes, F. Toscano, P. H. Souto Ribeiro, and S. P. Walborn, *Phys. Rev. A* **83**, 052325 (2011).
- [14] W. A. T. Nogueira, S. P. Walborn, S. Pádua, and C. H. Monken, *Phys. Rev. Lett.* **86**, 4009 (2001).
- [15] W. A. T. Nogueira, S. P. Walborn, S. Pádua, and C. H. Monken, *Phys. Rev. Lett.* **92**, 043602 (2004).
- [16] R. M. Gomes, A. Salles, F. Toscano, P. H. Souto Ribeiro, and S. P. Walborn, *Phys. Rev. Lett.* **103**, 033602 (2009).
- [17] R. M. Gomes, A. Salles, F. Toscano, P. H. Souto Ribeiro, and S. P. Walborn, *J. Opt.* **13**, 064020 (2011).
- [18] D. S. Tasca, S. P. Walborn, F. Toscano, and P. H. Souto Ribeiro, *Phys. Rev. A* **80**, 030101 (2009).
- [19] J. C. Howell, R. S. Bennink, S. J. Bentley, and R. W. Boyd, *Phys. Rev. Lett.* **92**, 210403 (2004).
- [20] D. S. Tasca, S. P. Walborn, P. H. Souto Ribeiro, F. Toscano, and P. Pellat-Finet, *Phys. Rev. A* **79**, 033801 (2009).
- [21] S. P. Walborn, A. Salles, R. M. Gomes, F. Toscano, and P. H. Souto Ribeiro, *Phys. Rev. Lett.* **106**, 130402 (2011).
- [22] P. B. Dixon, G. A. Howland, J. Schneeloch, and J. C. Howell, *Phys. Rev. Lett.* **108**, 143603 (2012).
- [23] J. Schneeloch, P. B. Dixon, G. A. Howland, C. J. Broadbent, and J. C. Howell, *Phys. Rev. Lett.* **110**, 130407 (2013).
- [24] M. D'Angelo, Y.-H. Kim, S. P. Kulik, and Y. Shih, *Phys. Rev. Lett.* **92**, 233601 (2004).
- [25] D. S. Tasca, S. P. Walborn, P. H. Souto Ribeiro, and F. Toscano, *Phys. Rev. A* **78**, 010304(R) (2008).
- [26] D. S. Tasca, L. Rudnicki, R. M. Gomes, F. Toscano, and S. P. Walborn, *Phys. Rev. Lett.* **110**, 210502 (2013).
- [27] R. M. Gomes, A. Salles, F. Toscano, P. H. S. Ribeiro, and S. P. Walborn, *Proc. Natl. Acad. Sci. USA* **106**, 21517 (2009).
- [28] L. K. Shalm, D. R. Hamel, Z. Yan, C. Simon, K. J. Resch, and T. Jennewein, *Nat. Phys.* **9**, 19 (2012).
- [29] K. Garay-Palmett, M. Corona, and A. B. U'Ren, *Revista Mex. Física S* **57**, 6 (2011).
- [30] M. Corona, K. Garay-Palmett, and A. B. U'Ren, *Opt. Lett.* **36**, 190 (2011).
- [31] J. Wen, P. Xu, M. H. Rubin, and Y. Shih, *Phys. Rev. A* **76**, 023828 (2007).
- [32] J. Wen, M. H. Rubin, and Y. Shih, *Phys. Rev. A* **76**, 045802 (2007).
- [33] J. Wen and M. H. Rubin, *Phys. Rev. A* **79**, 025802 (2009).
- [34] A. J. H. van der Torren, S. C. Yorulmaz, J. J. Renema, M. P. van Exter, and M. J. A. de Dood, *Phys. Rev. A* **85**, 043837 (2012).
- [35] J. Pan, D. Bouwmeester, M. Daniel, H. Weinfurter, and A. Zeilinger, *Nature* **403**, 515 (2000).
- [36] P. Walther, K. J. Resch, T. Rudolph, E. Schenck, H. Weinfurter, V. Vedral, M. Aspelmeyer, and A. Zeilinger, *Nature* **434**, 169 (2005).
- [37] C. K. Law and J. H. Eberly, *Phys. Rev. Lett.* **92**, 127903 (2004).
- [38] S. S. Straupe, D. P. Ivanov, A. A. Kalinkin, I. B. Bobrov, and S. P. Kulik, *Phys. Rev. A* **83**, 060302 (2011).
- [39] C. K. Hong, Z. Y. Ou, and L. Mandel, *Phys. Rev. Lett.* **59**, 2044 (1987).
- [40] S. P. Walborn, A. N. de Oliveira, S. Pádua, and C. H. Monken, *Phys. Rev. Lett.* **90**, 143601 (2003).
- [41] S. P. Walborn, W. A. T. Nogueira, A. N. de Oliveira, S. Pádua, and C. H. Monken, *Mod. Phys. Lett. B* **19**, 1 (2005).
- [42] P. van Loock and A. Furusawa, *Phys. Rev. A* **67**, 052315 (2003).
- [43] M. Edgar, D. Tasca, F. Izdebski, R. Warburton, J. Leach, M. Agnew, G. Buller, R. Boyd, and M. Padgett, *Nature Commun.* **3**, 984 (2012).